International Journal of Applied Engineering Research ISSN 0973-4562 Volume 12, Number 7 (2017) pp. 1383-1388
© Research India Publications. http://www.ripublication.com

Design of Outer Rotor Permanent Magnet Flux Switching Machine for Downhole Application

Rajesh Kumar[1*], Erwan Sulaiman[1], Laili Iwani Jusoh[1] and Fatihah Shafiqah Bahrim[1]

[1]Department of Electrical Power Engineering, University of Tun Hussein Onn Malaysia
Locked Bag 101, 86400 Parit Raja, Batu Pahat, Johor, Malaysia.

Abstract
Permanent magnet flux switching machine (PMFSM) has been a fascinating research interest for numerous applications over the last decades but few were developed for downhole application due to harsh environment. In this paper, a newly designed outer rotor permanent magnet flux switching machine with for downhole application is presented. Firstly, basic working principle and design topology of the outer-rotor PMFSM is introduced, then 2D finite-element analysis (FEA) model is developed to investigate the initial performance of machine at no-load and load condition. This proposed machine has an outer diameter of 50mm and stack length of 200mm can initially provide ~2.8 kW with an output torque of up to 21.08 Nm at base speed of 1271.52 rpm.

Keywords: Downhole application, permanent magnet, flux switching machine, finite element analysis, outer rotor, high torque.

INTRODUCTION

The bulk of oil and gas production in coming decades will be from the following two main resources

- Mature Fields
- Deep and Ultra Deep Reservoirs

The outcome from these mature fields is declining day by day and fields will be ceased permanently, if new methods for improving recovery, cost effective operation and maintenance are not put in place [1]. The price of typically fixed or floating platform for processing is increased significantly. Therefore, many deep sea fields may be worthless to develop.

Downhole processing, by moving the processing from surface or onshore to downhole can not only remove the top platforms or partly reduce the top area, but also upgrade productivity, ultimate restoration and improving efficiency whilst diminishing environmental impact.

Currently, Induction machine is widely utilized in downhole drilling because they are cost-effective, robust and easy to control [2]. Apart from this, induction machines are comparatively inefficient to its counter-part permanent magnet synchronous machine (PMSM) due to low efficiency and low torque density power density and low power factor [3]. Meanwhile, permanent magnet (PM) machines have almost same robustness and reliability with higher torque density, higher efficiency, higher flux density and smaller volume [4]. They are extensively used in industrial applications, but few were designed for downhole application due to high ambient temperature.

Today, with advancement in technologies and applications for magnetic material allows operation at higher surrounding temperatures without permanent magnetizations loss. Therefore, it is increasingly interesting trend for oil and gas sectors to design and manufacture PM machine having outer diameter is typically around 100mm constrained by the size of well but the axial length can be comparatively long [5]. A permanent magnet direct current (PMDC) downhole machine was proposed in [6]. The direct current is easily transmitted through PMDC to downhole by reducing the transmission losses. It is easy to control because it does not require variable frequency derive (VFD). However, it has few drawbacks such as the commutator system in PMDC not only introduces the complexity in manufacturing, extra losses over the brushes and also causes frequent failure. Furthermore, regular replacement is required every 2-3 years. In general, it is less reliable compared to a brushless synchronous machine. That is why; this kind of motor is restricted to onshore applications. In order to overcome the problem of brushes a permanent magnet synchronous machine was introduced in [7]. Along with high torque, it can also withstand to high temperature.

Today, flux switching machine have been proposed for different applications due to high torque and power density, larger electrical loading capability, low risk in demagnetization and better field weakening capabilities [8-10]. An inner rotor PMFSM has been developed for downhole application. It has advantages of both switch reluctance machine and PMSM. It is also proven that it has high efficiency, reliability and better cooling capability [11].

Accommodating the rotor on the outer surface will generate better torque, compared to the traditional inner rotor [12]. However, research on the PMFSM has mainly concentrated on the electromagnetic investigation and optimization of the inner rotor type with barely any attention given to the outer rotor PMFSM [13-15].

This paper concerns a comprehensive study of outer rotor PMFSM for downhole application. Initially, operating principle and design approach of proposed machine are discussed. Then, the no load and load analysis are investigated using 2D-FEA.

OPERATING PRINCIPLE

The fundamental principle of operation for outer rotor PMFSM has been described in [16]. Similarly, the same phenomenon is used in the proposed design.

In Fig.1, upper part is the laminated rotor identical to the switched reluctance machine (SRM). The lower of part of machine called as stator, comprises of armature winding and PM. The PM is located in between two stator teeth, and establishes a self-excited flux with a fixed direction within itself. In Fig.1 (a) when rotor pole aligns with the one of the stator teeth over which a coil is wound, the flux from PM is linked in the coil goes into the rotor pole. In Fig.1 (b) when rotor moves forward to align with the next stator teeth belongs to the same coil, the injected flux is drawn back to the stator tooth by the rotor pole, keeping the same amount of flux-linkage while reversing the polarity, i.e. accomplishing the flux-switching concept. Consequently, as the rotor rotates in forward direction, the flux linkage in the coils will change systematically, inducing back EMF. Therefore, if current is properly fed into the coils, an electromagnetic torque will be established, driving the rotor to move onward.

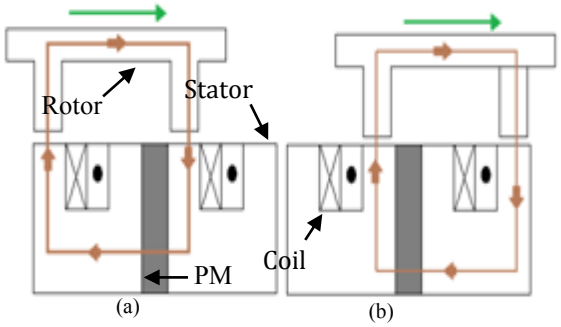

Figure 1: Operating principle of PMFSM

DESIGN TOPOLOGY

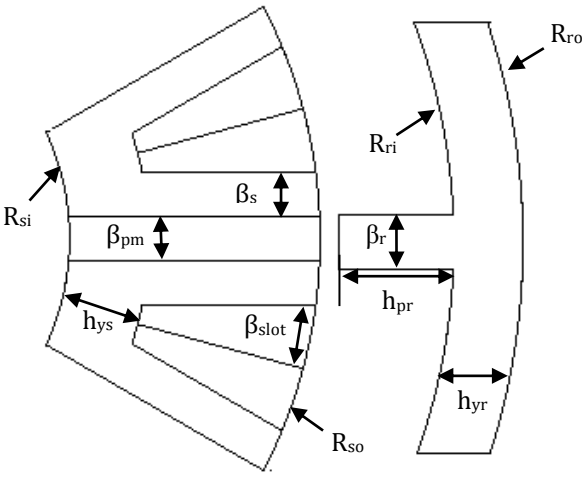

Figure 2: Key design parameters of outer rotor PMFSM

As shown in Fig-2, the basic design criterion for proposed outer rotor PMFSM are constrained by geometric relationships. Initially, permanent magnet width β_{pm} and stator tooth width β_s are chosen as

$$\beta_{pm} = \beta_s \quad (1)$$

In order to achieve sufficient rotor saliency, the rotor tooth height h_{pr}, is set as

$$h_{pr} = 1/6\ R_{ro} \quad (2)$$

On the other hand, additional relationship between stator outer radius R_{so}, stator inner radius R_{si} and stator back length hy_s, can be derived as

$$hy_s = R_{si}/\beta_s \quad (3)$$

$$R_{si} = R_{so}/2 \quad (4)$$

Therefore, ratio between stator inner radius and stator outer radius is 0.5. Moreover, coil number of each phase Nc is defined as

$$N_c = N_s/m \quad (5)$$

Where, m is the phase number and N_s is number of stator slot.

In addition, number of turns N can be derived as

$$N = A\alpha/\pi r^2 \quad (6)$$

Where, A is half slot area, r is radius of coil and α filling factor.

Moreover, the peak injected current I_m in each coil is

$$I_m = J_a\, \alpha\, A/N \quad (7)$$

Where, J_a is peak value of the current density in coils.

Furthermore, Finite Element Analysis (FEA) package, JMAG-Designer ver.14.0, developed by Japanese Research Institute (JRI) is employed as 2D-FEA solver for this proposed design. Neomax-35AH is utilized for PM material whose coercive force and residual flux density at 20C°, 932kA/m and 1.2T respectively while steel 35H210 is employed for rotor and stator part. The design restrictions and key parameters of outer rotor PMFSM are mentioned in Table I.

Finally, complete schematic of proposed design is shown in Fig.3, where polarities of PM are fixed in alternate direction, so it will yield 12 north and 12 south poles, while polarities of all the armature coils are specified in counter clockwise direction.

Table I. 12S-14P DESIGN PARAMETER

Parameters	Values
Stator Slots	12
Rotor Poles	14
Rotor Outer Radius	50mm
Rotor Inner Radius	36.7mm
Stator Outer Radius	36.2mm
Stator Inner Radius	18.1mm
Rotor Pole Height	8.3mm
Rotor Pole Width	3.9mm
Permanent Magnet Width	3.15mm
Stator Tooth Width	3.15mm
Slot Area	38.329mm^2
Stator Back Length	5.74mm
Rotor Yoke Length	5mm
Air Gap	0.5mm
Number of Turns	50
Machine Synchronous Speed	1000rpm
Current Density	10A/mm^2

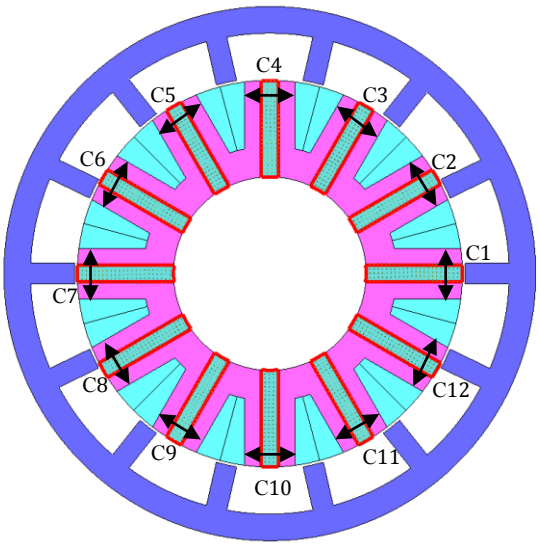

Figure 3: 12S-14P outer rotor PMFSM

OPEN CIRCUIT ANALYSIS

A. *Determination of Operating Principle*

The coil test arrangement is applied in order to affirm the principle operation of the prospective outer rotor PMFSM for downhole application. In a balanced three phase (3Ø) system, 3Ø of 12 armature coils are determined by inspecting and analyzing the magnetic flux linkage on each of armature coil.

For generating flux from PM only, the armature current density is fixed at 0A/mm^2. Therefore, at the speed of 1000r/min, the flux linkage on armature coils is shown in Table II.

Table II. FLUX REPRESENTATION OF ARMATURE COIL

Phase	Armature Coil
U	C3, C6, C9, C12
V	C2, C5, C8, C11
W	C1, C4, C7, C11

Once the polarity and phase of all the armature coil has been diagnosed, the 3Ø flux is sketched as shown in Fig.4. From the graph, it can be observed that the resulting amplitude of the PM generated flux is almost 0.18Wb with 90% sinusoidal waveform.

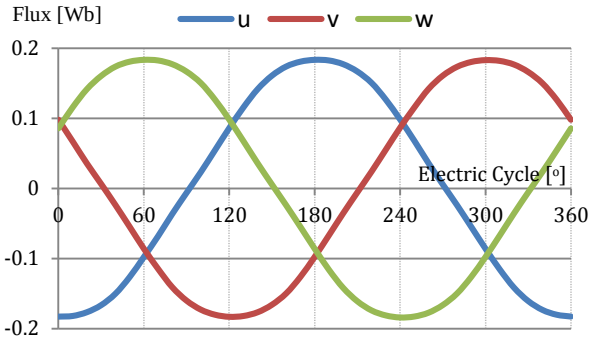

Figure 4: Three phase flux linkage

B. *Flux Lines Characteristics*

The following analysis involves the discussion of flux lines and flux density distribution for proposed structure. Figure.5 depicts that, the flux lines travel from stator teeth to rotor pole and return back from nearest rotor pole, in order to complete full cycles. Apparently, the initial design has more flux leakage, which distorts the flux flow from stator core to rotor and vice versa.

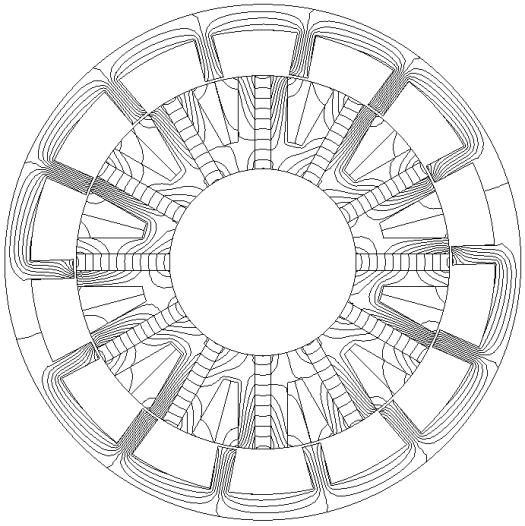

Figure 5: Outer rotor PMFSM flux lines

C. PM Flux Distribution

The objective of flux distribution is to monitor the field saturation effect on the machine. In Fig.6, the most of PM generated flux flows from stator to rotor and return back through next rotor teeth by generating a full flux cycle. In addition to that, the flux density configuration shows that the maximum value measured at around 2.39T.

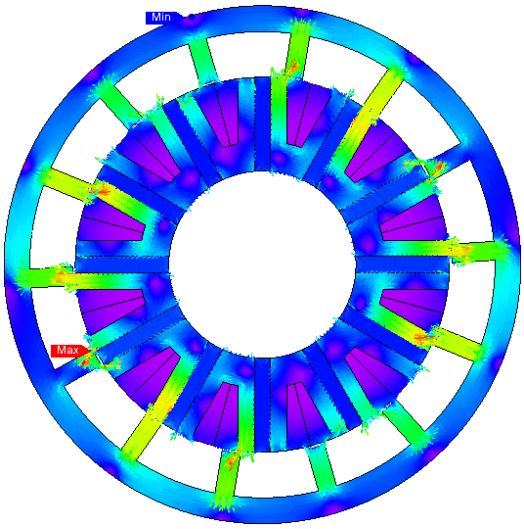

Figure 6: Flux distribution of 12s-14p

D. Cogging Torque

It is also called as detent or no-current torque. It is an undesirable component for machine operation. Therefore, the number of cycles for cogging torque can be derived as

$$N_p = N_r/HCF\ [N_r,N_s] \quad (8)$$

$$N_e = N_p\, N_s/N_r \quad (9)$$

Where, N_r denotes the number of rotor poles, HCF is the highest common factor, N_p is the constant, N_e is the number of cogging torque cycles.

The PM generated cogging torque analysis for one electric cycle is displayed in Fig.7. It is observed that the peak to peak cogging torque is about 8.5Nm. Moreover, the resulting waveform has 6 numbers of cycles.

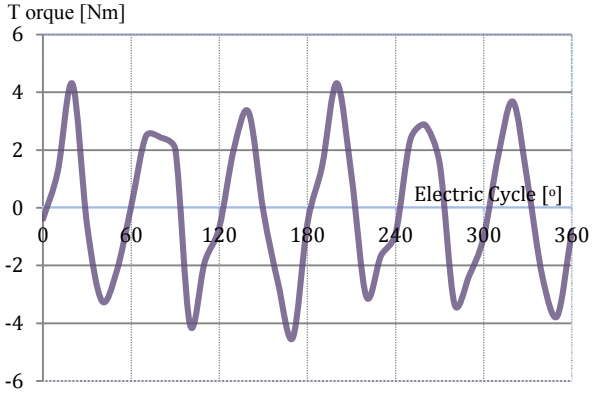

Figure 7: Cogging torque waveform

E. Induced Voltages

By revolving the rotor at rated speed of 1000r/min, no-load back Emf of the proposed configuration is illustrated in Fig.8. Initially, line and phase voltages of proposed design are approximately 500V and 289V respectively. The high back Emf is due to armature reaction, which creates demagnetizing effect in the machine. Therefore, by using design refinement techniques and optimization methods, the induced voltages of the initial design can be reduced into an acceptable condition. In spite of this, it has computed waveform exhibits a more favorable sinusoidal feature.

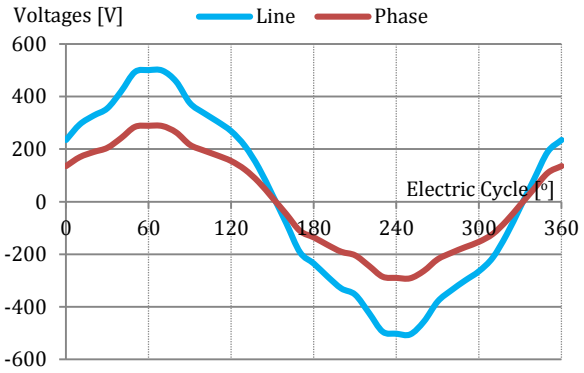

Figure 8: Induced voltages at 1000r/min

SHORT CIRCUIT ANALYSIS

A. Torque at Various Armature Current Density

The output torque of propose outer rotor PMFSM is analyzed at various armature current density. The obtained results are plotted in Fig.9, in which armature current density is varied from 0A/mm^2 to 10A/mm^2.

Initially, the proposed design is unable to achieve the specified target for downhole application. Thus, it can be improved through optimization.

However, the linearity in the graph shows that output torque is directly proportional to the armature current density and the maximum torque of 21.08 Nm is obtained when armature current density is set at 10A/mm^2.

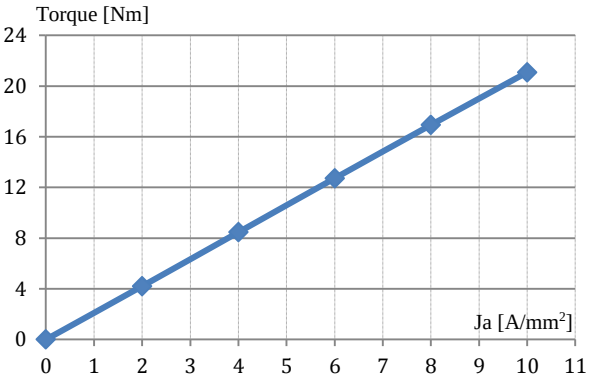

Figure 9: Torque versus various armature current densities

B. Torque- Power versus Speed Characteristics

Torque and power versus speed graph of the initial outer rotor PMFSM for downhole application is plotted in Fig.10. The solid green line indicates the torque-speed curve, while blue line represents the power curve. For proposed design, at base speed 1271.52 rpm, the torque obtained is 21.08 Nm. At maximum torque, the corresponding maximum power obtained from preliminary design is 2.8 kW.

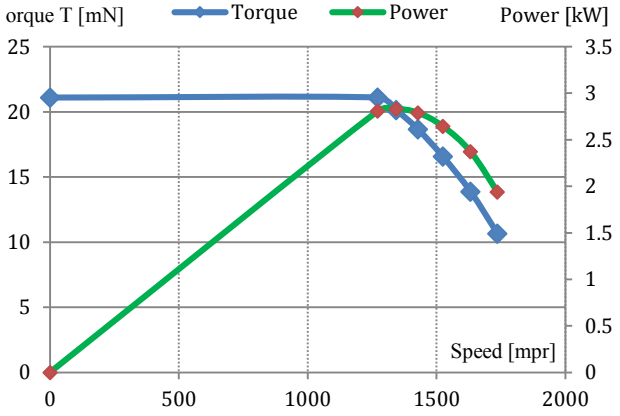

Figure 10: Torque-power against speed curve

CONCLUSION

The design study and corresponding result analysis of the proposed outer rotor PMFSM has been discussed and examined in this paper through 2-D FEA approach. Basically, the principles of operation, armature coil phase and polarity have been verified.

The performances of the proposed motor at no load and load condition such as cogging torque, flux lines, flux distribution, induced voltages, torque at various armature current density and torque-speed against power have also been investigated and exhibited. From the results obtained, it is expected that the motor will successfully achieve the targeted performances by further design refinement and optimization.

ACKNOWLEDGMENT

This research work is promoted by Research, Innovation, Commercialization and Consultancy Management (ORICC) UTHM, Parit Raja, Johor under vote number U519.

REFERENCES

[1]. A. Chen, R. B. Ummaneni, R. Nilssen and A. Nysveen (2008). Review of electrical machine in downhole application and the advantages. 13th international power electronics and motion conference, Poznan, Poland, September 2008.

[2]. M. W. Hooker, C. S. Hazelton, K. S. Kano and M.L. Tupper (2010). High temperature electrical insulation for EGS downhole equipment. Proceeding 35th workshop on geothermal reservoir engineering, Stanford, California, February 2010.

[3]. A. Chen, R. Nilssen and A. Nysveen (2010). Performance comparisons among radial flux, multistage transversal flux and three phase transverse flux PM machine for downhole application. IEEE transaction of industry application, pp. 779-789, January 2010.

[4]. M. J. Melfi, S. Evon and R. Mcelveen (2009). Induction versus permanent magnet motors. IEEE industrial application magazine, pp. 28-35, November-December 2009.

[5]. A. Chen, R. Nilssen and A. Nysvenn (2010). Investigation of a three phase flux switching permanent magnet machine for downhole application. 20th International conference on electrical machines, Rome, September 2010

[6]. M. Solesa and V. Sagalovskiy (2007). Direct current motors with permanent magnets – more downhole flexibility. MEALF, Sultanate of Oman, February 2007.

[7]. Z. Bingyi, L. Bingxue, F. Guihong and Z. Fuyu (2007). Research of multipolar permanent magnet synchronous submersible motor for screw pump. International conference on mechatronics and automation, Harbin, China, August 2007.

[8]. C. S. Walter, H. Polinder, J. A. Ferreira (2013). High-torque-density high efficiency flux switching machine for aerospace applications. IEEE journal of emerging and selected topics in power electronics, vol. 1, no. 4, pp. 327-336, December 2013.

[9]. E. B. Sulaiman, T. Kosaka (2013). Development of high torque and high power density hybrid excitation flux switching motor for traction drive in hybrid electric vehicles. Energy and Power Engineering, pp. 446-454, September 2013.

[10]. J. Ojeda, M. G. Simoes, G. Li, and M. Gabsi (2012). Design of a flux-switching electrical generator for wind turbine systems. IEEE.Trans, vol. 48, no. 6, pp. 1808-1816, November-December 2012.

[11]. A. Chen (2011). Investigation of permanent magnet machines for downhole applications. Ph.D thesis, NTNU, Trondheim, Norway, January 2011.

[12]. C. V. Aravind, M. Norhisam, I. Aris, D. Ahmad and M. Nirei (2011). Double rotor switched reluctance motors: fundamentals and magnetic circuit analysis. IEEE SCORED, Kualalumpur, pp. 294-299, January 2011.

[13]. A. Zulu, B. C. Mecrow and M. Armstrong (2012). Permanent magnet flux switching synchronous motor employing a segmental rotor. IEEE. Trans, vol. 48, no. 6, pp.2259-2267, November-December 2012.

[14]. Z. Q. Zhu, Y. Pang, D. Howe, S. Iwasaki, R. Deodhar and A. Pride (2005). Analysis of electromagnetic performance of flux-switching permanent-magnet machines by nonlinear adaptive lumped parameter magnetic circuit model.

IEEE.Trans. J. Magn, vol. 41, no. 11, November 2005.

[15]. J. X. Shen and W. Z. Fei. Permanent magnet flux switching machines topologies, analysis and optimization. 4th international conference on power engineering, energy and electric derives, Istanbul, Turkey, May 2013.

[16]. Y. Wang, M. J. Jin, J. X. Shen W. Z. Fei, P. C. K. Luk (2010). An outer-rotor flux-switching permanent magnet machine for traction applications. IEEE energy conversion congress and exposition, pp. 1723 – 1730, September 2010.